Analysis of Variations on Land Surface Temperature (LST) and Total Column Water Vapor (TCWV) in East Java using Sentinel-3 Satellite

Wijayanti, R. F.,[1] Handoko, E. Y.,[2*] Syariz, M. A.,[2] Kurnyawati, P.,[2] Putra, A. P.,[3] Hamzah, S.,[1] Tjaronge, M. W.,[1] Bakri, B.[1] and Gafur, M. Y. S.[1]
[1]Department of Civil Engineering. Universitas Hasanuddin, Indonesia
[2]Department of Geomatics Engineering, Institut Teknologi Sepuluh Nopember (ITS), Indonesia
E-mail: ekoyh@its.ac.id*
[3]Department of Fisheries Agribusiness, Universitas Dr Soetomo, Indonesia
**Corresponding Author*

DOI: https://doi.org/10.52939/ijg.v21i7.4315

Abstract

The study of spatiotemporal variations of Land Surface Temperature (LST) and Total Column Water Vapor (TCWV) in East Java Province from 2021 to 2023 using Sentinel-3 SLSTR satellite imagery is the subject of this research. This study aims to assess the seasonal climate dynamics in the tropical monsoon region and evaluate the statistical relationship between LST and atmospheric water vapour content. The remote sensing data from the Sea and Land Surface Temperature Radiometer (SLSTR) were processed to produce multi-temporal LST and TCWV maps. Furthermore, the Split-Window Algorithm was utilized to obtain LST, while TCWV was obtained using the Ocean and Land Colour Instrument (OLCI) through differential absorption techniques. The data analysis employed a combination of temporal aggregation, spatial mapping techniques, and simple linear regression to evaluate the relationship between LST and TCWV. The results indicate that seasonal variations are significant. LST values peak during the dry season, particularly in September 2023, coinciding with the El Niño-induced drought, and TCWV reaches its maximum during the wet season. However, the statistical relationship between the two variables is weak, with a coefficient of determination (R^2) of 0.022. This suggests that only 2.2% of LST variability can be explained by TCWV, indicating the presence of more influential surface and atmospheric factors, including land cover, vegetation density, and topographic complexity. The results of this study demonstrate the utility of Sentinel-3 data for regional climate monitoring and indicate the limitations of utilizing TCWV as the primary predictor of LST variability. The conclusions of this study demonstrate the necessity for an integrated multiparameter approach in future drought and climate assessments in the tropics.

Keywords: Climate Monitoring, Land Surface Temperature (LST), Seasonal Variation, Sentinel-3 SLSTR, Total Column Water Vapor (TCWV)

1. Introduction

East Java is one of the provinces in Indonesia that occupies the most significant area on the island of Java. The province of East Java is characterised by a tropical climate, with an average temperature of 27.1°C in 2021 [1], 25°C in 2022 [2], and 27.2°C in 2023 [3]. In addition to determining the characteristics of seasonal climate patterns, especially in the monsoon region in East Java, Indonesia, further studies are required on what affects it, such as Land Surface Temperature (LST) and Total Column Water Vapor (TCWV). LST is defined as the land surface temperature that occurs due to radiation, and it is considered to be the most reliable estimate of the Earth's thermodynamic temperature [4]. Furthermore, LST is one of the parameters employed to determine climate change and hydrological balance at local and global scales [5]. Meanwhile, TCWV is a vertically integrated parameter of water vapour content in the atmosphere and plays an essential role in regulating latent heat flux, cloud formation, and precipitation cycles [6] and [7].

East Java is a monsoon-influenced region that experiences apparent seasonal variations. These variations are characterised by elevated temperatures and decreased precipitation during the dry season (June-September) and increased rainfall during the rainy season (November-March). Therefore, the East Java region is an appropriate location for a research case study to investigate how surface temperature and atmospheric humidity evolve temporally and interact statistically.

The development of contemporary remote sensing technology has enabled numerous satellites to provide data for monitoring climate and environmental variables over a wide range of temporal and spatial scales. One such example is the Sentinel-3 satellite image, in which the Sentinel-3 satellite is utilised to collect data from the Sea and Land Surface Temperature Radiometer (SLSTR) instrument, which provides Land Surface Temperature data, and the Ocean and Land Colour Instrument (OLCI), which provides Total Column Water Vapor (TCWV) data [8] and [9]. Several studies have used Sentinel-3 data for monitoring climate, hydrology, and land surface process. These studies include research on improving LST accuracy using the single-channel algorithm (SC), the split-window algorithm (SW), and four machine-learning models on the Tibetan Plateau [10]. The study utilised Sentinel-3 imagery, incorporating three climate parameters: Land Surface Temperature (LST), Fractional Vegetation Cover (FVC), and Total Column Water Vapour (TCWV), to investigate the monitoring of drought [11], The integration of both terrestrial and atmospheric indicators has been demonstrated to be an effective method for the assessment of both droughts and climate [12]. In East Java, the primary focus of climate monitoring is frequently directed towards precipitation, as indicated by the Normalised Difference Vegetation Index (NDVI), and vegetation [13][14] and [15] Nevertheless, the temporal relationship between LST and TCWV is seldom considered. Furthermore, the assumption of linear correlation may not fully capture the complex interactions shaped by ENSO events, topographic heterogeneity, and land use dynamics [6] and [16]. Therefore, this study analyses the temporal variation of LST and TCWV in East Java from 2021 to 2023 and evaluates the statistical relationship (R^2) between LST and TCWV.

2. Methodology

2.1 Research Location

The research location of this study is East Java, Indonesia. The area of East Java is 47,803.49 km^2. East Java Province is between 7°07′12″ South Latitude and 8°28′48″ South Latitude and 111°00′00″ East Longitude and 114°24′ East Longitude. Furthermore, the Java Sea borders East Java Province to the north, the Bali Strait to the east, the Indian Ocean to the south, and Central Java Province to the west. The research location in East Java is shown in Figure 1.

2.2 Remote Sensing Data

The present study employs remote sensing data, specifically Sentinel-3 satellite images captured. Sentinel-3 features three instruments: the Sea and Land Surface Temperature Radiometer (SLSTR), the Ocean and Land Colour Instrument (OLCI), and the Altimetry Surface Topography Mission (STM) [8].

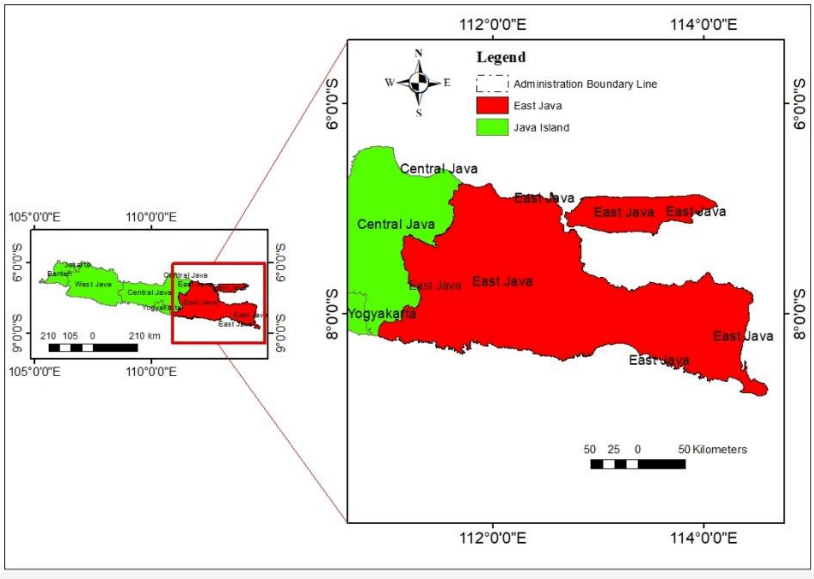

Figure 1: East Java, Indonesia

Further, this research used Sentinel-3 SLSTR to provide the essential data. Sentinel-3 SLSTR was created utilizing a conical scanning imaging radiometer and the along-track scanning dual-view approach to provide robust atmospheric correction throughout a dual-view swath [17]. The 10.8 μm channel's dynamic range has been extended, and the specially designed 3.7 μm detectors enable flames at ~650 K without saturation [18]. Land Surface Temperature (LST) and Total Column Water Vapor (TCWV) values were obtained from Sentinel-3 SLSTR data. Sentinel-3 represents a fundamental element of the European Space Agency's (ESA) Copernicus Programme, specifically engineered to facilitate global environmental and climate monitoring [8].

Land Surface Temperature (LST) retrieval on the Sentinel-3 SLSTR satellite requires knowledge of pixel emissivity. Furthermore, the algorithm used for daytime and night-time LST retrieval varies on this Sentinel-3 SLSTR satellite: daytime retrieval uses Visible and Near-Infrared (VNIR), while night-time retrieval uses Split Window (SW) [19]. Consequently, there are differences in LST values between daytime and nighttime retrieval. Furthermore, the accuracy of the LST value is affected by factors such as the amount of vegetation and the number of clouds present at the time the image was captured [4]. LST products from the Sentinel-3 SLSTR were obtained using the Split-Window (SW) algorithm, which utilises the brightness temperatures of the thermal infrared bands centred at 10.8 μm and 12.0 μm (referred to as T_{11} and T_{12}). The SW method is employed to correct atmospheric absorption, primarily resulting from water vapour, by calculating a linear combination of the two channels [9].

The Land Surface Temperature (LST) with a Split-window Algorithmic process is presented about the Sentinel-3 SLSTR L2 data, as illustrated in Equation 1 [17] and [18]:

$$T = a_{f,i,wvc} + b_{f,i}(T_{11} - T_{12})^{\sec\left(\frac{\theta}{m}\right)} + \left(b_{f,i} + c_{f,i}\right)T_{12}$$

Equation 1

The following is an explanation of equation 1 above, where T is *LST*, T_{11} is the brightness temperature on the satellite viewing angle 11 m, T_{12} is the brightness temperature on the satellite viewing angle 12 m, m is the viewing angle, $a_{f,i,wvc}$ is an algorithm coefficient that according of vegetation fraction (f), surface biome (i), WVC, and day/night time, $b_{f,i}$ and $c_{f,i}$ is algorithm coefficient depends on vegetation fraction (f) and surface biome (i).

The TCWV values are derived from Sentinel-3 imagery, specifically from the Ocean and Land Colour Instrument (OLCI), utilising the near infrared channel in the 940 nm water vapour absorption band. The method employs a differential absorption technique, which involves the extraction of the water vapour signal through a comparison of radiance in the absorbing and non-absorbing bands [19] and [20]. TCWV retrieval on heterogeneous surfaces is challenging in surface applications due to surface reflectance variability. To address this issue, Sentinel-3 utilises atmospheric correction models and radiative transfer simulations to mitigate the retrieval bias. Furthermore, the multi-angle observations from SLSTR enhance the retrieval of atmospheric parameters by accounting for surface anisotropy [18].

TCWV values are expressed in kg/m², representing the atmosphere's vertically integrated water vapour content. Monthly composites were generated using daily granules and employing temporal smoothing and spatial mosaics under cloud-free conditions to represent seasonal trends in water vapour concentration over East Java. The LST and TCWV data were recorded monthly from 2021 to 2023 and obtained from the https://browser.dataspace.copernicus.eu/ website. Monthly averages pertinent to drought monitoring were calculated.

2.3 Statistical Model

This section utilises the coefficient of determination (R^2) to process the data following Sentinel-3 LST and TCWV modelling. The R-squared metric evaluates how accurately the model aligns with the observed data. In this instance, R-squared is utilised to assess the variability in the dependent variable (LST) that can be attributed to the independent variable (TCWV) based on simple linear regression. Moreover, the R-squared value ranges from 0 to 1. In this study, a value of 0 indicates that the independent variables do not explain the variability in the dependent variable, and a value of 1 indicates a perfect fit between the models. Equation 2 is used to determine the R^2 [21] and [22]:

$$R^2 = 1 - \frac{\sum\left(y - \hat{y}\right)^2}{\sum\left(y - \bar{y}\right)^2}$$

Equation 2

Where y is the observed response variable, $\hat{y}$ is the predicted value that is commensurate with the given data, and $\bar{y}$ is the mean of the observed response variable.

2.4 Research Flowchart

The research flowchart for this study is divided into several steps (Figure 2). The primary data for this research is Sentinel-3 SLSTR satellite imagery, with data obtained monthly from 2021 to 2023. The first step is reprojecting each Sentinel-3 SLSTR Satellite Imagery fit from the East Java projection system. This component is significant because the Sentinel-3 SLSTR satellite imagery-oriented view capture requires data reorientation to align with the actual north direction, ensuring the image has a coordinate system that matches the exact location on Earth.

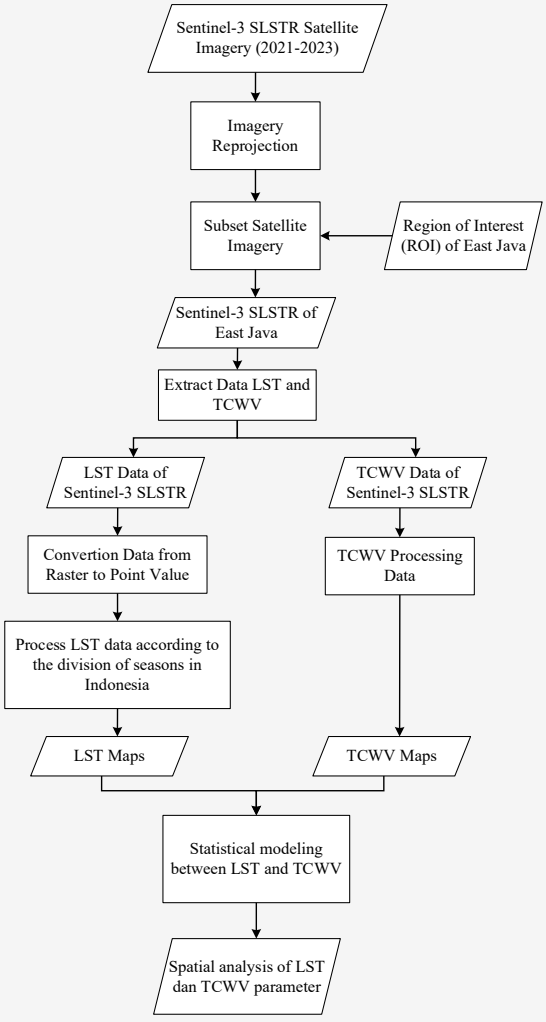

Figure 2: LST and TCWV modeling

The second step is to subset Sentinel-3 SLSTR satellite imagery to fit the ROI of East Java. Furthermore, the Sentinel-3 SLSTR satellite imagery provides the required data for this research: LST and TCWV. Therefore, the LST and TCWV data from Sentinel-3 SLSTR Satellite Imagery are extracted. On LST data, conversion to Point Value determines the average monthly Land Surface Temperature (LST).

Furthermore, the LST value was originally in Kelvin and converted to Celsius, as the unit is often employed in temperature measurements. Moreover, the LST data processing and the LST of each month also help divide the monsoon in Indonesia to determine droughts indicated in different seasons. Further, TCWV data processing is carried out. Furthermore, following the acquisition of LST and TCWV data and maps for each month from 2021 to 2023, calculations and correlation analysis were conducted between the LST and TCWV data. This was undertaken to ascertain the adequacy of the model, specifically to determine the extent to which the independent variable influenced the dependent variable, employing the R-squared parameter.

3. Results and Discussion

This study uses Sentinel-3 SLSTR data with LST and TCWV parameters for drought monitoring in East Java, and analyzes the relationship between these parameters. The results and discussion of the study are presented below.

3.1 LST conditions in East Java

The data processing results in this study indicate that multi-temporal Land Surface Temperature (LST) variations from 2021 to 2023 in East Java exhibit different seasonal characteristics due to the monsoon climate in East Java. As illustrated in Figure 3, the lowest average LST is observed in February 2022, reaching 18.07 °C. This coincides with the peak of the rainy season in East Java. This period represents the peak of the rainy season in Indonesia, with increased rainfall and cloud cover contributing to a decrease in land surface heating due to reduced solar radiation [10]. Moreover, the maximum LST was recorded in September 2023 at 37.57°C, coinciding with this region's dry period. High LST values are indicative of reduced soil moisture and lack of rainfall during the dry period, hence increasing ground surface heating [23].

The factors influencing the level of LST in East Java are local hydrometeorological conditions and the El Niño-Southern Oscillation (ENSO) phenomenon, a large-scale climate driver. During the occurrence of the El Niño phenomenon, surface warming due to suppressed convective activity causes a decrease in rainfall and an increase in solar insolation [15]. The extreme LST in September 2023 can partly be attributed to the El Niño phenomenon, which manifested in East Java. This climatic event served to intensify drought conditions across numerous regions in Indonesia [24].

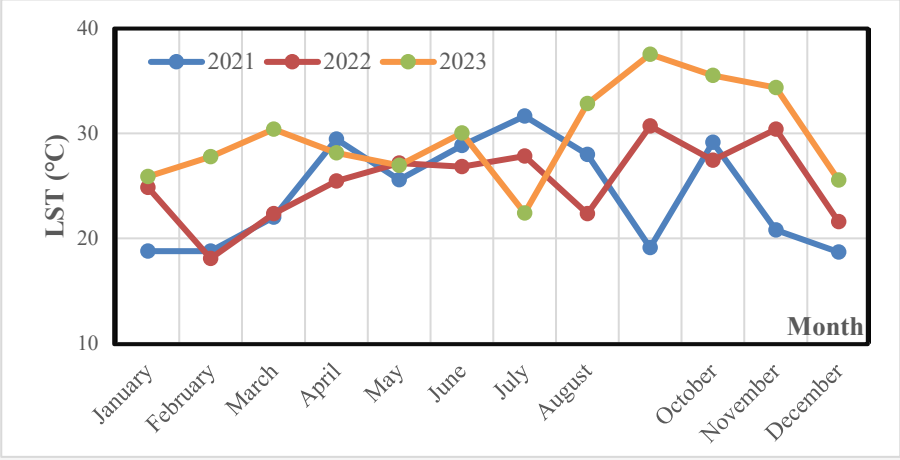

Figure 3: Land Surface Temperature (LST) chart in East Java

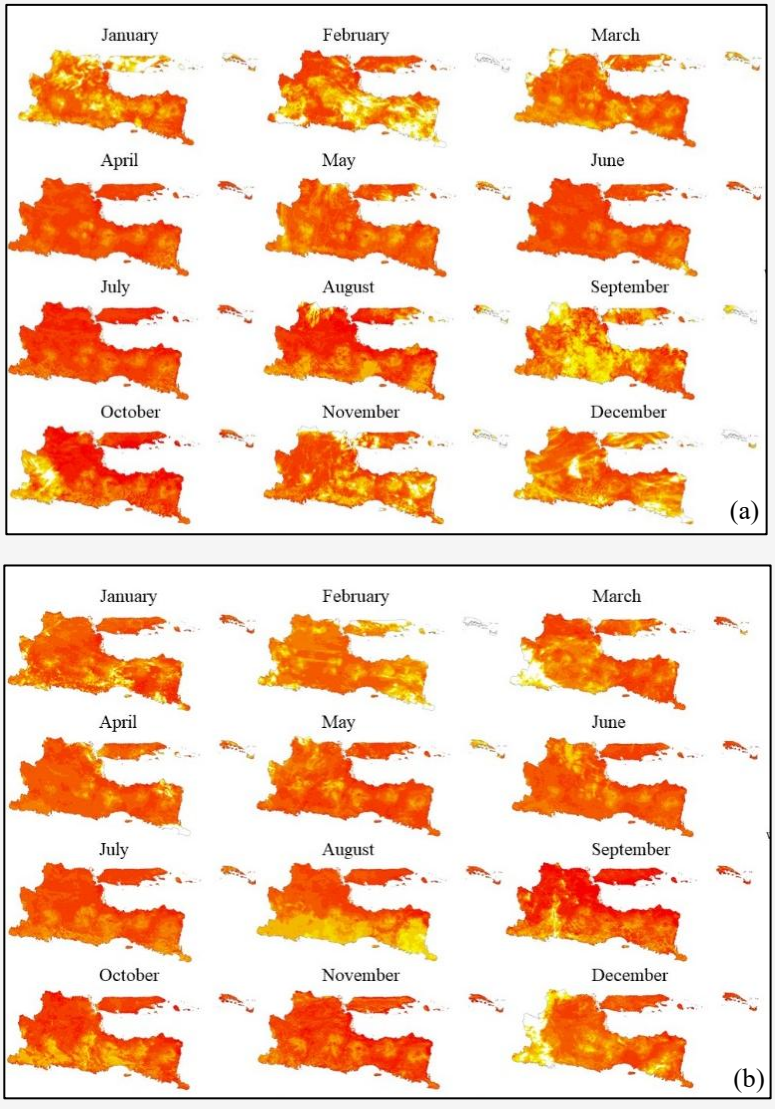

Figure 4: Monthly Land Surface Temperature (LST) Maps in East:
(a) 2021, (b) 2022 (Continue next page)

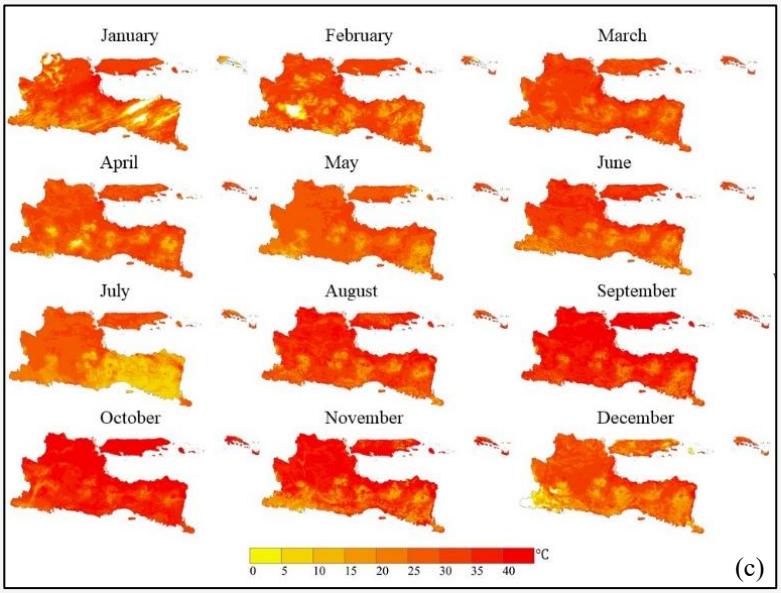

Figure 4: Monthly Land Surface Temperature (LST) Maps in East: (a) 2021, (b) 2022, and (c) 2023
(Continue from previous page)

Figure 4 illustrates LST's spatial and temporal distribution in East Java from 2021 to 2023. During this period, the LST map consistently exhibited elevated average LST levels from July to September, coinciding with the dry season in Indonesia. Furthermore, the study results demonstrate that most regions within East Java are represented on the LST map in dark red, indicating LST values over 35°C, with certain hotspots surpassing 40°C. Considering climatological factors, it is evident that this distribution pattern manifests during the dry season.

This is characterised by heightened solar heating and evapotranspiration deficits, which result in an augmentation of land surface temperatures. During the rainy season, identifying LST data from satellite imagery is subject to certain limitations. This study indicates that, from November to March, coinciding with the rainy season in East Java, there is a conspicuous absence of LST values greater than 10 °C, suggesting anomalously low temperatures. The presence of this event is indicated on the LST map due to the presence of a light yellow or orange hue, potentially attributable to cloud contamination within the thermal infrared band of the Sentinel-3 SLSTR image [15] and [18]. The analysis of spatiotemporal LST trends revealed that the most extreme thermal conditions characterised 2023 during the study period, which is of significant concern for surface hydrology and drought risk. The observed patterns emphasise the necessity of integrating seasonal and interannual climate variability (e.g. ENSO) into the drought risk assessment framework [8] and [20].

3.2 TCWV Conditions in East Java

The following section presents a map showing the distribution of the total column water vapor (TCWV) values in East Java. Water vapor concentrations are related to regional climate and rainfall patterns. Figure 5 depicts the TCWV map for each month in East Java from 2021 to 2023. Figure 5 depicts the TCWV distribution value in East Java from 2021 to 2023, varying from 0 kg/m² (light blue) to more than 60 kg/m² (dark blue). Further, the lower the TCWV number, the greater the possibility of drought due to insufficient water vapor in the area. From 2022 to 2023, the TCWV of June to August has values ranging from 20 to 30 kg/m², which is lower than in other months. Therefore, it marked the beginning of the dry season. Furthermore, this seasonal pattern suggests that water vapor levels are highest at the beginning and end of the year and lowest in the middle months, representing the changing rainy and dry seasons in East Java. This might have been related to seasonal fluctuations in rainfall and temperature, which influence the amount of water vapor in the atmosphere. *3.3 Correlation Value Between LST and TCWV in East Java Province*

The analysis of the data processing results indicates a weak linear relationship between Land Surface Temperature (LST) and Total Column Water Vapour (TCWV) in East Java during the 2021-2023 period. The coefficient of determination (R^2) obtained from the regression model is 0.022, indicating that only 2.2% of the variability of LST can be explained by fluctuations in TCWV.

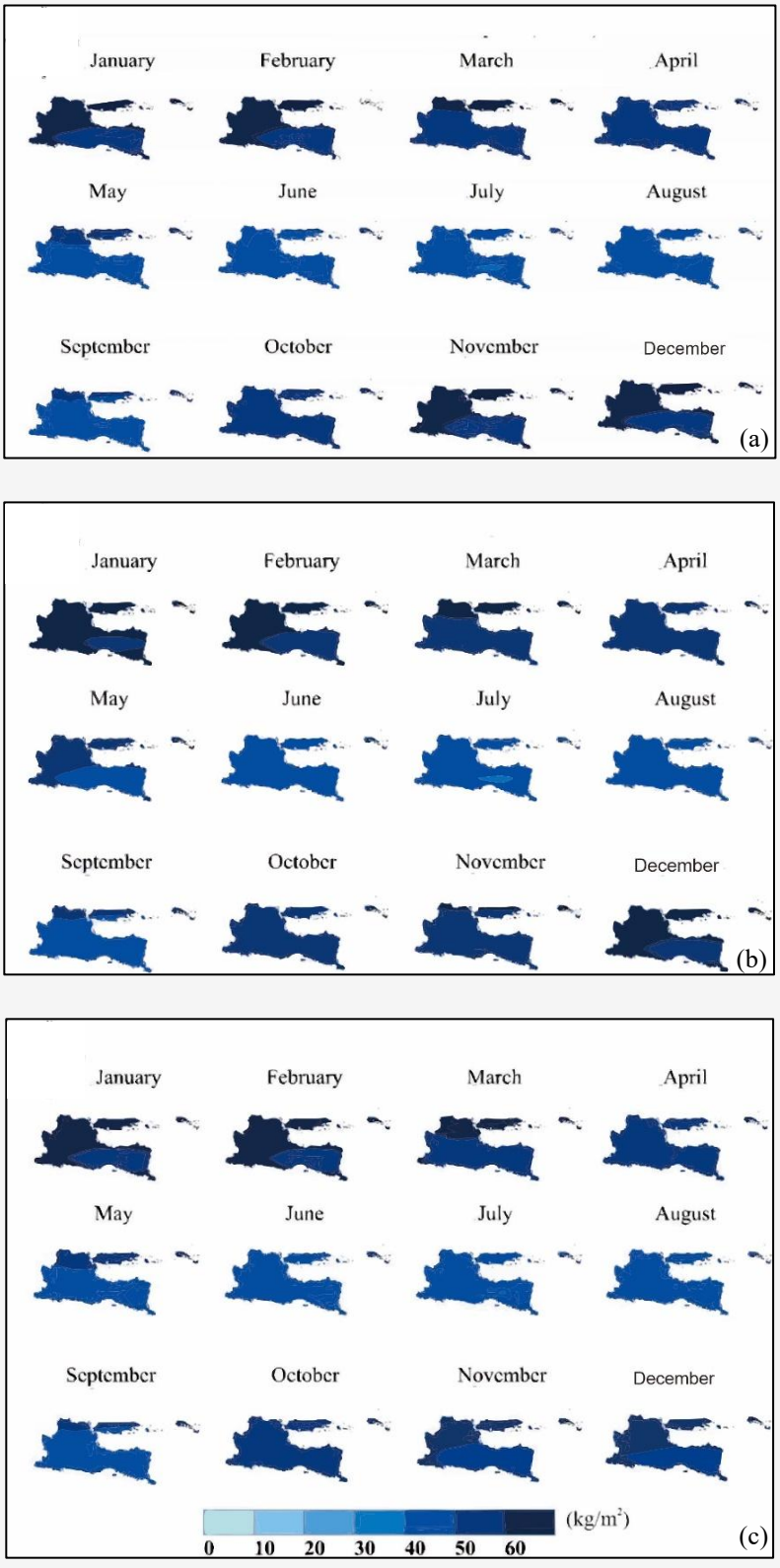

Figure 5: Monthly Total Column Water Vapor (TCWV) in East Java: (a) 2021, (b) 2022, and (c) 2023

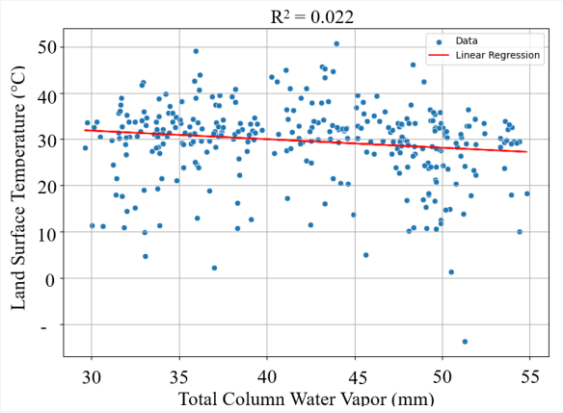

Figure 6: R-squared between LST and TCWV parameters 2021-2023 in East Java

This finding suggests that TCWV does not primarily govern LST variability in the study area. The weak relationship is due to the complex interactions between various environmental and anthropogenic factors that affect surface temperature. These factors include land cover type, urban expansion, topography, vegetation density, and radiant energy balance.

There is some seasonal and spatial overlap between TCWV and LST, such as increased humidity during the rainy season, coinciding with moderate LST. However, the statistical relationship between the two parameters remains minimal. High TCWV values are frequently associated with dense cloud cover, where high cloud counts can reduce solar radiation reaching the ground surface and thus contribute to lower LST. Therefore, the relationship between LST and TCWV is negative or inversely proportional. Therefore, although TCWV contributes significantly to atmospheric processes, its impact on LST is constrained by the tropical monsoon in East Java. As illustrated in Figure 6, the dispersed nature of the data points reflects TCWV's limited predictive capability for LST in this region.

4. Conclusion

This study examines the spatiotemporal variations in Land Surface Temperature (LST) and Total Column Water Vapour (TCWV) over East Java from 2021 to 2023 using Sentinel-3 SLSTR satellite data. The findings indicate discernible seasonal characteristics, with LST at its maximum during the dry season (predominantly September 2023) and TCWV at its maximum during the wet season. The reverse seasonal trend observed between LST and TCWV indicates the monsoonal climate system characterising East Java. This study utilises spatiotemporal analyses to examine the impact of extreme climate events, such as El Niño, on surface heating patterns. The highest LST recorded in September 2023 coincided with an El Niño episode, which exacerbated drought stress in the region. The TCWV distribution map confirmed the suppression of atmospheric moisture during this period, amplifying the regional hydrometeorological anomaly.

Although seasonal patterns can be observed, the statistical relationship between LST and TCWV was weak in this study. The simple linear regression analysis findings yielded an R^2 value of 0.022, indicating that TCWV can explain 2.2% of the variation in LST. Therefore, it suggests that TCWV, when considered independently, is not a strong predictor of surface thermal conditions in East Java. The weak correlation can be attributed to the combined influence of other surface parameters, including land cover, vegetation density, urbanisation, topography, and radiation flux. These parameters collectively have a more dominant control on surface temperature dynamics.

Therefore, although LST and TCWV demonstrate significant seasonal patterns, their mutual relationship is not statistically significant in this study. To facilitate more accurate future assessments of climate and drought, it is recommended that multivariable analyses incorporating vegetation indices (NDVI), land-use categories, and meteorological inputs be integrated. This approach will enhance our understanding of the complexity of surface-atmosphere interactions in tropical environments. This study emphasises the value of Sentinel-3 SLSTR remote sensing data in detecting regional climate variations. It also highlights the limitations of using TCWV to interpret LST dynamics in heterogeneous tropical environments.

Acknowledgements

We would like to thank Institut Teknologi Sepuluh Nopember and Universitas Hasanuddin for their support of this research.

References

[1] Badan Pusat Statistik Provinci Java Timur (2022). Provinsi Jawa Timur dalam Angka 2022 [Jawa Timur Province in Figures 2022]. [Online]. Available: https://jatim.bps.go.id/en/publication/2022/02/25/33699f6fcd84e0e2a0ad96f0/provinsi-jawa-timur-dalam-angka-2022.html. [Accessed: Sept. 21, 2024].

[2] Badan Pusat Statistik Provinci Java Timur (2023). Provinsi Jawa Timur dalam Angka 2023 (Jawa Timur Province in Figures 2023). [Online]. Available: https://jatim.bps.go.id/en/publication/2023/02/28/446036fbb58d36b0092

12dbc/jawa-timur-province-in-figures-2023.html. [Accessed: Sept. 21, 2024].

[3] BPS. (2024). Provinsi Jawa Timur dalam Angka 2024 (Jawa Timur Province in Figures 2024). [Online]. Available: https://jatim.bps.go.id/en/publication/2024/02/28/53a51c3ca566561a72d10bde/jawa-timur-province-in-figures-2024.html. [Accessed: Sept. 21, 2024].

[4] Ghent, D., Singh, J., Veal, K. and Remedios, J., (2024). The Operational and Climate Land Surface Temperature Products from the Sea and Land Surface Temperature Radiometers on Sentinel-3A and 3B. *Remote Sensing,* Vol. 16(18). https://doi.org/10.3390/rs16183403.

[5] Wang, Z., Sui, L. and Zhang, S., (2022). Generating Daily Land Surface Temperature Downscaling Data Based on Sentinel-3 Images. *Remote Sensing,* Vol. 14(22). https://doi.org/10.3390/rs14225752.

[6] Perondi, D., Fraisse, C, W., Watson, J, A., Boote, K, J., Zotarelli, L. and Huffaker, R. G., (2023). Assessing the Impact of Sowing Dates and ENSO in a Drought Index-based Insurance for Soybean. *Climate Risk Management,* Vol. 41. https://doi.org/10.1016/j.crm.2023.100544.

[7] Preusker, R., Henken, C, C. and Fischer, J., (2021). Retrieval of Daytime Total Column Water Vapour from OLCI Measurements Over Land Surfaces. *Remote Sensing*, Vol. 13. https://doi.org/10.3390/rs13050932.

[8] Clerc, S., Donlon, C., Borde, F., Lamquin, N., Hunt, S. E., Smith, D., McMillan, M., Mittaz, J., Woolliams, E., Hammond, M., Banks, C., Moreau, T., Picard, B., Raynal, M., Rieu, P. and Guerou, A., (2020). Benefits and Lessons Learned from The Sentinel-3 Tandem Phase. *Remote Sensing*, Vol. 12(17). https://doi.org/10.3390/RS12172668.

[9] Planells, L, P., Niclòs, R., Puchades, J., Coll, C., Göttsche, Frank-M., Valiente, José A., Valor, E. and Galve, J. M., (2021). Validation of Sentinel-3 SLSTR Land Surface Temperature Retrieved by the Operational Product and Comparison with explicitly Emissivity-Dependent Algorithms. *Remote Sensing,* Vol. 13(11). https:// doi.org/10.3390/rs13112228.

[10] Qi, Y., Zhong, L., Ma, Y., Fu, Y., Wang, X. and Li, P., (2023). Estimation of Land Surface Temperature Over the Tibetan Plateau Based on Sentinel-3 SLSTR Data. *IEEE Journal of Selected Topics in Applied Earth Observations and Remote Sensing,* Vol. 16. https://doi.org/10.1109/JSTARS.2023.3268326.

[11] Musyimi, P, K., Sahbeni, G., Timár, G., Weidinger, T. and Székely, B., (2023). Analysis of Short-Term Drought Episodes Using Sentinel-3 SLSTR Data under a Semi-Arid Climate in Lower Eastern Kenya. *Remote Sensing*, Vol. 15(12). https://doi.org/10.3390/rs15123041.

[12] Liu, Q., Zhang, S., Zhang, H., Bai, Y. and Zhang, J., (2020). Monitoring Drought Using Composite Drought Indices Based on Remote Sensing. *Science Total Environment*, Vol. 711. https://doi.org/10.1016/j.scitotenv.2019.134585.

[13] Samanta, S. (2024). Identification of Agricultural Drought through Vegetation Health Analysis at Erap Station under the Markham Valley of Papua New Guinea. *International Journal of Geoinformatics*, Vol. 20(11), 106–115. https://doi.org/10.52939/ijg.v20i11.3691

[14] Preedapirom, P., Robert, O., Onchang, R., and Jeefoo, P. (2024). Drought Monitoring Using MODIS Satellite-Based Data in Kamphaeng Phet Province, Thailand. *International Journal of Geoinformatics*, Vol. 20(1), 1–11. https://doi.org/10.52939/ijg.v20i1.3019.

[15] Wei, W., Zhang, J., Zhou, L., Xie, B., Zhou, J. and Li, C., (2021). Comparative Evaluation of Drought Indices for Monitoring Drought Based on Remote Sensing Data. *Environmental Science Pollution Research*, Vol. 28(16). https://doi.org/10.1007/s11356-020-12120-0.

[16] Shi, L., Schreck, C, J. and Schröder, M., (2018). Assessing the Pattern Differences between Satellite-Observed Upper Tropospheric Humidity and Total Column Water Vapor during Major El Niño Events. *Remote Sensing*, Vol. 10(8). https://doi.org/10.3390/rs10081188.

[17] ESA. (2012). *Sentinel-3: ESA's Global Land and Ocean Mission for GMES Operational Services*. European Space Agency. Netherlands

[18] Castelli, E., Casadio, S., Papandrea, E., Pettinari, P., Valeri, M., Achilli, A., Bojkov, B.R., Di Roma, A., Perfetti, C., Dinelli, B.M. (2025). AIRWAVE-SLSTR An Algorithm to Estimate the Total Column of Water Vapour from SLSTR Measurements over Liquid Surfaces. *Remote Sensing*. Vol. 17; 1205. https://doi.org/10.3390/rs17071205.

[19] Nie, J., Ren, H., Zheng, Y., Ghent, D. and Tansey, K., (2021). Land Surface Temperature and Emissivity Retrieval from Nighttime Middle-Infrared and Thermal-Infrared Sentinel-3 Images. *IEEE Geoscience and Remote Sensing Letters*, Vol. 18(5). https://doi.org/10.1109/LGRS.2020.2986326.

[20] Chang, S., Chen, H., Wu, B., Nasanbat, E., Yan, N. and Davdai, B., (2021). A Practical Satellite-Derived Vegetation Drought Index for Arid and Semi-Arid Grassland Drought Monitoring. *Remote Sensing,* Vol. 13(3). https://doi.org/10.3390/rs13030414.

[21] Kv¥lseth, T. O., (2014). Cautionary Note About R^2. *American Statistician*, Vol. 39(4). https://doi.org/10.1080/00031305.1985.10479448.

[22] Alexander, D. L., Tropsha, A. and Winkler, D. A., (2015). Beware of R^2: Simple, Unambiguous Assessment of the Prediction Accuracy of QSAR and QSPR Models. *Journal of Chemical Information and Modeling*, Vol. 55(7). https://doi.org/10.1021/acs.jcim.5b00206.

[23] Thammaboribal, P. (2024). Investigating Land Surface Temperature Variation and Land Use Land Cover Changes in Pathumthani, Thailand (1997-2023) using Landsat Satellite Imagery: A Comprehensive Analysis of LST and Urban Hot Spots (UHS). *International Journal of Geoinformatics*, Vol. 20(2), 27–41. https://doi.org/10.52939/ijg.v20i2.3063.

[24] BMKG. Anomali Suhu Udara Rata-rata Tahunan [Annual Average Air Temperature Anomaly]. [Online]. Available: https://www.bmkg.go.id/iklim/?p=ekstrem-perubahan-iklim#:~:text=Berdasarkan data dari 91 stasiun adalah sebesar 27.0 °C. [Accessed: Sept. 21, 2024].